

## A Simulation-Optimization Model for “Air Sparging” and “Pump and Treat” Groundwater Remediation Technologies

K. Sookhak Lari<sup>1,\*</sup> and H. Safavi<sup>2</sup>

<sup>1</sup>*Environmental and Water Resource Engineering Research Group, Department of Civil and Environmental Engineering, Imperial College, London SW7 2AZ, UK*

<sup>2</sup>*Department of Civil Engineering, Isfahan University of Technology, Isfahan 8415683111, Iran*

Received 12 July 2007; revised 4 December 2007; accepted 1 January 2008; published online 2 September 2008

**ABSTRACT.** Using a new concept of sub-period, a simulation-optimization model for initial evaluation of air sparging (AS) and pump-and-treat (PAT) groundwater remediation technologies is presented in order to facilitate the study of aquifers contaminated with soluble volatile organic compounds. The new simulation and optimization process assumes a specific type of contaminant and a homogeneous soil texture. The simulation module connects two existing models (MODFLOW and MT3DMS) to Henry's Equation. Simulation is performed by dividing the simulation period into sub-periods and using Henry's equation for each sub-period. An optimization module minimizes the cost of the remediation using an objective function subjected to quality and quantity constraints, and derived using a classic form of genetic algorithm. In addition to demonstrating how to solve a typical problem using the optimization module, we demonstrate field application of the simulation module for an aquifer near the Tehran Refinery, which is contaminated by methyl tertiary-butyl ether. One constraint for this problem is that installation of remediation equipment is prohibited in urban areas. Due to this constraint, AS wells must be positioned upward the urban area. Therefore, these wells act as a barrier that restricts contaminant flow downward into the city. The results of the simulation show the advantages of employing simultaneous remediation technologies.

*Keywords:* pump-and-treat, air sparging, simulation, optimization, remediation

### 1. Introduction

Petroleum compounds account for a large proportion of groundwater contaminants in some areas (Khan, 2004). These compounds include a wide range of light and heavy hydrocarbons with a range of physical and chemical properties. A group of petroleum compounds called "volatile organic compounds" (VOCs) has serious harmful effects on human health. These compounds have a boiling temperature less than 250 °C and a Henry constant greater than  $10^{-5}$  (Benner et al., 2000; Bass et al., 2000). Highly water-soluble VOCs often don't appear in non-aqueous phase liquid (NAPL) form in groundwater and instead travel in solution as a result of water movement through an aquifer. Leakage of these compounds into groundwater is common in both developed and developing countries (Benner et al., 2000; DLA, 2005). Pump-and-treat (PAT) and air sparging (AS) technologies can be used to remediate aquifers contaminated with VOC solutions (Khan et al., 2004).

The PAT process consists of extracting contaminated water from the ground using a network of pumping wells, treat-

ing the water, then returning it to the ground. In addition to its application for soluble VOCs, PAT can be used to treat other types of contaminants, depending on the hydro-geological conditions (Khan et al., 2004; Erickson et al., 2002). In contrast, the AS approach is only used to treat VOCs. This technology is based on air injection into the aquifer and physical contaminant removal based on Henry's Law (i.e. that the amount of a gas in solution depends on both the partial pressure of the gas and its solubility); once the contaminant is forced from the groundwater, it is collected by means of some form of vapor extraction system, and treated using other processes such as biological degradation (Khan et al., 2004).

The equations that govern the simulation of a PAT process for soluble contaminants are the Boussinesq and mass transport equations for porous media (Harbaugh et al., 2000; Zheng and Wang, 1999). Therefore, field-scale PAT simulation techniques have been developed based on advances in methods for finding numerical solutions for differential equations (Wang and Anderson, 1982). Some powerful models for PAT simulation and optimization are also now available. Examples include the United States Geological Survey's modular three-dimensional finite-difference flow model, MODFLOW, and the three-dimensional modular solute-transport model MT3DMS (Harbaugh et al., 2000; Zheng and Wang, 1999, 2002).

The mass transport phenomena that occur during AS are

---

\* Corresponding author. Tel.: +44(0) 20 7594 6018; fax: +44(0) 20 7594 6124. E-mail address: ksookhak@imperial.ac.uk (K. Sookhak Lari).

considerably more complicated. To define the equations that govern the AS process, multi-phase systems must be developed. Depending on the required accuracy, analytical, lumped-parameter, and compartmentalized equations may be generated to simulate AS technology (McCray, 2000). Different models of the AS process have been proposed depending on the type of the differential equations selected for the simulation. For example, the T2VOC model employs numerical solutions of analytical multi-phase equations (McCray, 2000; Falta et al., 1995).

Although analytical equations are very accurate, employing these equations for field-scale simulation of AS faces serious problems. The large number of calculations required and the need for a range of input data are two of the most significant problems (McCray, 2000; Falta et al., 1995). On the other hand, lumped- and compartmentalized-parameter methods are commonly used to simulate field-scale AS applications. This approach requires fewer calculations, and has the advantages of providing sufficient accuracy to guide engineering designs and of being relatively easy to use (Benner et al., 2000; McCray, 2000). One equation that provides sufficient field-scale accuracy for use with the lumped-parameter model is the Henry equation (McCray, 2000).

Some researchers have suggested the simultaneous application of AS and PAT in aquifers contaminated with soluble VOCs (Khan et al., 2004). However, despite these suggestions, simulation models capable of modeling the simultaneous application of these techniques are rare (McCray, 2000).

In the present study, we have proposed a simulation-optimization model for combined use of AS and PAT based on certain logical assumptions that are required for field-scale application of the model. To accomplish this, we combined the MODFLOW and MT3DMS models with the Henry equation by means of a new method of intercommunication between the modules of the model. The effectiveness of the simulation module and the possibility of intercommunication between modules are requirements to produce an effective optimization module.

## 2. Simulation Method

### 2.1. Assumptions

In addition to various physical and chemical principles that must be considered in PAT and AS application, the most important assumption during simulation is that the horizontal distribution of the AS air will be small compared to the dimensions of the problem area being treated. Several studies have attempted to validate this assumption in homogeneous or semi-homogeneous soils. For example, Johnson et al. (1993) and Ahlfeld et al. (1994) studied semi-homogeneous soils and found that with a pressure of 5 to 30 kPa above hydrostatic pressure in the diffusers, the maximum horizontal air distribution would be about 1 m from the point of injection. The empirical studies of N.R. Thomson and his colleagues (Thomson and Johnson, 2000; Thomson et al., 2000), which were also based on analysis of simulations, showed that in homogene-

ous soils, horizontal growth of the air zone is fairly impossible comparing to the plume size. In their studies, Lesson et al. (1995) observed that the majority of airflow at the surface of an aquifer composed of homogeneous sand was within a 0.3- to 0.6-m radius around the injection point. LaBrecque and Lundergaard (1998) showed that within a relatively homogeneous sand, the steady-state air distribution was centered around the sparg point, with an estimated maximum air saturation of between 20 and 40%. A similar air distribution was reported by McKay and Acomb (1996).

In contrast, studies of heterogeneous soils, including gravelly sediments and silty sands, showed that the horizontal distribution of the air zone is higher than in homogeneous soils, and that horizontal movement of air channels greatly decreases AS performance (LaBrecque and Lundergaard, 1998; Thomson and Johnson, 2000).

### 2.2. Governing Equations

The governing equation describing three-dimensional movement of groundwater assuming constant density (i.e. the Boussinesq equation) is as follows (Harbaugh et al., 2000):

$$\frac{\partial}{\partial x} \left( K_{xx} \frac{\partial h}{\partial x} \right) + \frac{\partial}{\partial y} \left( K_{yy} \frac{\partial h}{\partial y} \right) + \frac{\partial}{\partial z} \left( K_{zz} \frac{\partial h}{\partial z} \right) + W = S_s \frac{\partial h}{\partial t} \quad (1)$$

where  $K_{zz}$ ,  $K_{yy}$ , and  $K_{xx}$  are the hydraulic conductivity along the Z, Y, and X directions, respectively ( $L T^{-1}$ );  $W$  is the volumetric flow rate of fluid sink/source per unit volume of the aquifer ( $L^{-1}$ );  $h$  is the hydraulic head in the aquifer (L);  $S_s$  is specific storage ( $L^{-1}$ );  $t$  represents time (T). This equation is solved by the MODFLOW model.

The partial differential equation that describes three-dimensional solute transport in groundwater is (Zheng and Wang, 1999):

$$\frac{\partial}{\partial x_i} \left( \theta D_{ij} \frac{\partial C}{\partial x_j} \right) - \frac{\partial}{\partial x_i} (q_i C) + q_s C_s + R = \frac{\partial(\theta C)}{\partial t} \quad (2)$$

where  $C$  is the solute concentration ( $M L^{-3}$ );  $D_{ij}$  is the hydrodynamic dispersion coefficient ( $L^2 T^{-1}$ );  $C_s$  is the concentration of fluid sink/source ( $M L^{-3}$ );  $\theta$  is the porosity of the aquifer;  $q_s$  is the Darcy flux ( $L T^{-1}$ );  $R$  is a chemical reaction term ( $M L^{-3} T^{-1}$ ). This equation is solved by the MT3DMS model.

The equation describing Henry's law is (McCray, 2000; USAF, 2002):

$$C_{GAS} = C_{WATER} \times H \times CC \quad (3)$$

where  $C_{GAS}$  is the contaminant concentration in the diffusing air ( $M L^{-3}$ );  $C_{WATER}$  is the contaminant concentration in water ( $M L^{-3}$ );  $H$  is Henry's dimensionless coefficient;  $CC$  is a dimensionless contact coefficient between the air and water, and must be determined empirically. Since  $CC$  is a bulk parameter, several properties and coefficients of the model can be com-

combined to represent this parameter. In other words, effects of parameters like specific enthalpy, density and viscosity on VOC removal during aeration can be combined into a single, bulk parameter (i.e.  $CC$ ) by means of experimental evaluations.

### 2.3. Description of the Simulation Method

The basis of the simulation performed by our simulation-optimization model is division of the mass transfer design period into sub-periods. This new concept allows the initial production of a hydraulic model for the design period for the aquifer. This is achieved by solving equation 1 inside the MODFLOW model. After MODFLOW verifies the hydraulic head and the velocity field, the MT3DMS model solves equation 2 for the first sub-period. After the analysis is complete for the first sub-period, the contaminant concentrations in nodes that contain AS wells are decreased using the corresponding concentration values in equation 3. The concentration values in all nodes, including the AS well nodes, are then applied as initial concentration values for use in the next sub-period. This procedure is continued until the end of the simulation period.

This simulation algorithm is sensitive to the length of sub-period: the shorter the sub-period, the more accurate the result. Modelers can use a simple, practical technique to select the appropriate sub-period. In this technique, a conventional MODFLOW/MT3DMS simulation (i.e. one without equation 3 or the use of sub-periods) is initially applied to the aquifer and the pumping wells. The modeler then selects an arbitrary sub-period, and uses the new simulation algorithm described in the present paper for the aquifer and the pumping wells. If the results of the two both simulations are sufficiently close, the sub-period can be used in the simulation-optimization model. If not, a shorter sub-period is selected and the comparison is repeated iteratively until an acceptable value of the sub-period is obtained. In this technique, selecting an appropriate sub-period is obviously related to the accuracy required by the engineering design and depends on the designer's judgment.

Due to the specific format of the input and output files used by the MT3DMS model (i.e. .BTN files), automatic modification of contaminant concentration values at the end of each sub-period is possible. This process is applied inside the file (Zheng and Wang, 1999). One of the main roles of the .BTN files is to verify the initial values of contaminant concentration used in the mass transfer model. Because the simulation-optimization model must be able to finalize a series of simulations independently of the user during an iterative optimization process, we used the MODFLOW2000 and MT3DMS4b versions of the simulation models. Automatic modification of the values is made possible by using .BAT files in these versions of the software (Zheng and Wang, 1999).

### 3. Optimization Method

In this study, we used genetic algorithm (GA) as the optimization algorithm for simultaneous use of AS and PAT technologies. This algorithm is a random search algorithm, which

offers strong advantages when dealing with complex, multi-variable objective functions. The advantages of this algorithm include a low probability of occurrence of local extremes, easier encoding, and easy application of various types of constraints compared with alternatives such as gradient-based optimization models (Gen and Cheng, 1997). The application of various types of random search models for PAT optimization, such as GA, has been increasingly reported by researchers in recent years (e.g. Erickson et al., 2002; Guan and Aral, 1999; Spiliotopoulos et al., 2004). In addition, some powerful GA optimization models for PAT technology have been presented. One of these models, which is completely compatible with MODFLOW and MT3DMS, is the Modular Groundwater Optimization (MGO) model (Zheng and Wang, 2002). To take advantage of this compatibility, we based the PAT-AS optimization module in the present study on the ideas of MGO model.

The applied objective function in the AS-PAT optimization module is a cost-minimization function that can be described as follows:

$$J = \text{Min} \left( \sum_{i=1}^m a_i + \sum_{i=1}^n k \cdot b_i + \sum_{i=1}^m c_i + \sum_{i=1}^n k \cdot d_i \right) \quad (4)$$

where  $i$  represents the number of wells of a given type ( $n$  and  $m$  indicate the number of AS and PAT wells, respectively);  $a$  represents the construction cost of each PAT well;  $b$  represents the construction cost of each AS well;  $c$  represents the total pumping and treatment cost for each PAT well;  $d$  represents the air injection cost for each AS well;  $k$  represents the value of an activation indicator for each AS well (i.e. whether a given well is active). Where an AS well is active,  $k = 1$ ; if not,  $k = 0$ . In this objective function, the treatment cost of the contaminated water can only be estimated as a percentage of the pumping cost, regardless of the contaminant concentration.

Quantity constraints on the optimization problem take the form of the maximum allowable pumping rate and the quality constraint is the maximum allowable contaminant concentration in a specified area. These constraints are defined as follows:

$$0 < P_{\text{well}} < P_{\text{max}} \quad (5)$$

$$0 < C_{\text{area}} < C_{\text{max}} \quad (6)$$

where  $P_{\text{well}}$  is the pumping rate for a specific well;  $P_{\text{max}}$  is the maximum allowable pumping rate for that well;  $C_{\text{area}}$  is the contaminant concentration in a given area;  $C_{\text{max}}$  is the maximum allowable contaminant concentration in that area.

Based on the nature of this objective function, the decision variable for an AS well is its activation status (i.e. whether it is active or turned off).

Every chromosome of the GA in this study consists of  $M$  groups named  $P_i$  ( $i = 1, 2, \dots, M$ ) and  $M$  groups of  $A_i$  ( $i = 1, 2, \dots, M$ ). The  $P$  groups verify the PAT wells whereas the  $A$  groups verify the  $R$  values of the AS wells, where  $R$  equals the integer of  $n$  divided by  $m$  ( $m$  and  $n$  are the numbers of PAT

and AS wells, respectively).

In this type of chromosome, the number of AS wells must be equal to or greater than the number of PAT wells. If the true residual of  $n / m$  is shown by  $res$  ( $res < m$ ), then each group of  $A$ , from 1 to  $res$ , will take an extra gene. The arrangement of groups  $A$  and  $P$  inside a typical chromosome in the GA is shown in Figure 1.

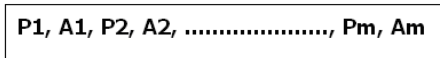


Figure 1. Groups A and P in a typical chromosome.

In general, the precision applied to the pumping rate for PAT wells is defined as follows (Zheng and Wang, 2002):

$$dQ = Q_{max} / (N - 1) \text{ for } N = 2^g \quad (7)$$

where  $Q_{max}$  is the maximum allowable pumping rate in PAT wells;  $N$  is the number of possible pumping rate values within the pumping rate interval (i.e. within the range of permissible pumping rates);  $dQ$  is the pumping rate precision, and  $g$  is the number of genes in each  $P$  group. For example, if each PAT well is determined by 5 genes, the number of possible values for pumping rate will be  $2^5 = 32$  and  $dQ = Q_{max} / 31$ .

In the  $A$  groups, each gene determines one of the AS wells. If the determined AS well is active (on), the value of the related gene is 1; if not, it will be 0. The values for crossover and mutation in the GA are usually empirical (Gen and Cheng, 1997; Guan and Aral, 1999). Therefore, the possibility of changing these values to match available empirical data is considered in the simulation-optimization model, and the effect of these values during the optimization procedure is selected following the selection rules in the MGO model (Zheng and Wang, 2002). A flowchart for the optimization module is shown in Figure 2.

#### 4. Model Performance

##### 4.1. Sensitivity and Stability of the Simulation Module

###### 4.1.1. Scope

We evaluated the stability and sensitivity of the simulation module against changes of input parameters during a problem. In this problem, the sensitivity of the numerical solution to the hydraulic and mass transfer equations (i.e. equations No. 1 and 2), using the sub-period concept, was analyzed. In this section, we compared several responses of both MODFLOW /MT3DMS and the presented model, subjected to same situations.

The parameters that we assessed in this problem were hydraulic conductivity, porosity, boundary conditions and the sub-period length.

###### 4.1.2. Description of the Problem

Consider an unconfined rectangular aquifer as shown in

figure 3. hydraulic boundary conditions of this aquifer consist of constant head at left and right sides of it. the boundary condition of contamination is a region of constant concentration. Figure 3 shows location of boundary conditions.

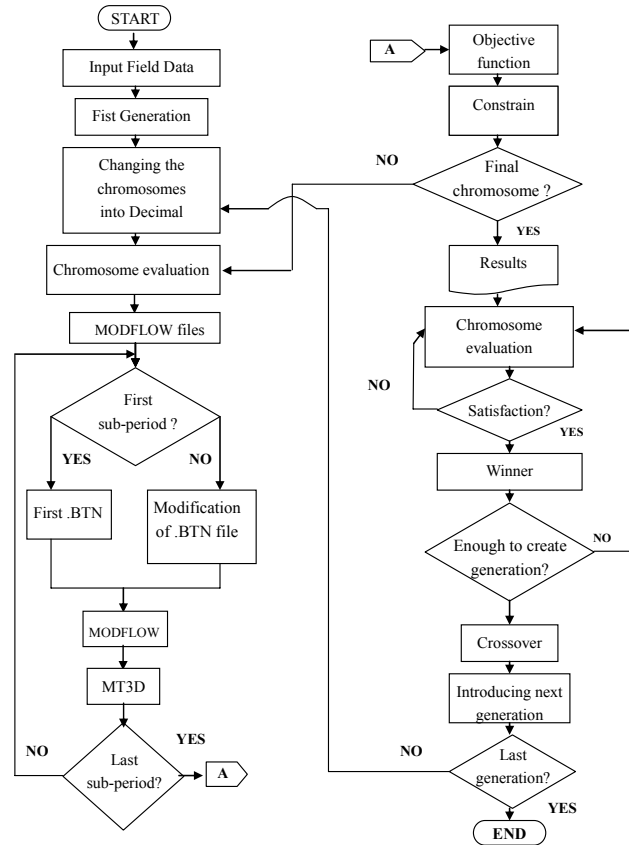


Figure 2. Optimization module flowchart.

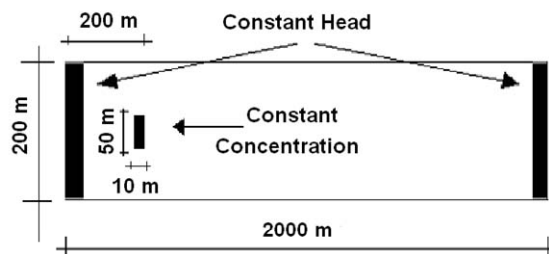


Figure 3. The conceptual view of the problem.

Based on the conceptual view in figure 3, we defined parameters of the problem in a way that five separate states could be created. Table 1 represents these five states. According to the table, states  $S_2$  to  $S_5$  are similar to  $S_1$  except one of their parameters. These parameters include hydraulic conductivity coefficient, porosity, concentration of the mass source and constant head of the left hand boundary condition.

For this problem, we selected the length of the simulation period to be 2000 days and evaluated the extension of conta-

**Table 1.** Representation of Various States of the Problem

| State | Hydraulic Conductivity Coefficient, $k$ (m/d) | Porosity | Constant Concentration (mg/L) | Left Hand Constant Head (m) | Right Hand Constant Head (m) |
|-------|---|----------|-------------------------------|-----------------------------|------------------------------|
| S1    | 10  | 0.5      | 5000                          | 40                          | 20                           |
| S2    | 10  | 0.5      | 10000                         | 40                          | 20                           |
| S3    | 5   | 0.5      | 5000                          | 40                          | 20                           |
| S4    | 10  | 0.3      | 5000                          | 40                          | 20                           |
| S5    | 10  | 0.5      | 5000                          | 50                          | 20                           |

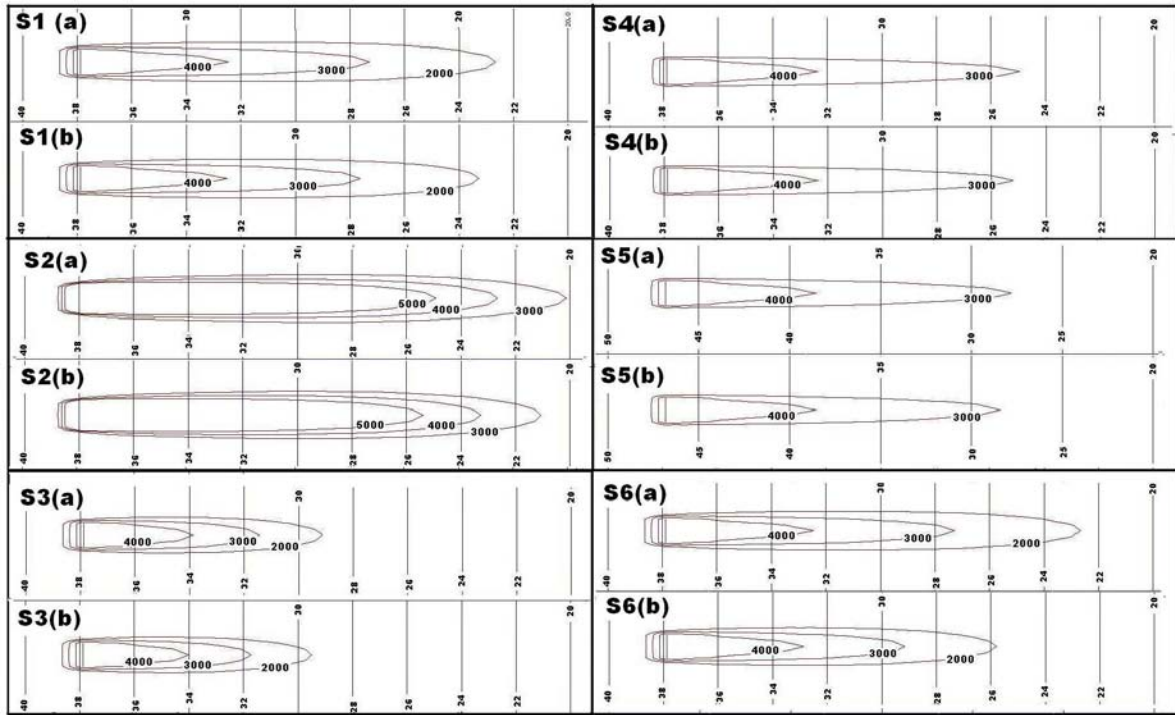


**Figure 4.** Results of simulations using MODFLOW/MT3DMS and the presented model.

mination plume after this period for all five states. Two different methods were implemented to simulate this problem. First, MODFLOW/MT3DMS model solved each of the five states. We denoted these results with “a” index (for example,  $S1(a)$  represents simulation of  $S1$  state using MODFLOW/MT3DMS model). Then each of these five states was simulated using the presented model and a 2-day sub-period. In this case, we denoted each result with “b” index (for example,  $S1(b)$  represents simulation of  $S1$  state using presented model and a 2-day sub-period).

In addition, we designed a separate state, named  $S6$ , to evaluate the effect of sub-period length on the results. This state is completely similar to  $S1$  state in respect of input data. The only difference is that  $S6$  was simulated using presented model for both indexes. We used a 5-day sub-period for  $S6(a)$  and a 20-day sub-period for  $S6(b)$ .

#### 4.1.3. Results

Figure 4 shows results of all simulations using MODFLOW/MT3DMS and presented model. According to the figure, there

is no significant difference between simulations of two models in  $S1$  to  $S5$  states. In other words, the 2-day sub-period is a suitable assumption for this example in respect of changes in hydraulic and boundary conditions.

For the  $S6$  state, 5-day and 20-day sub-periods were implemented for “a” and “b” indexes respectively. According to the figure, plume extension for the 5-day sub-period has an acceptable compatibility with the result of MODFLOW/MT3DMS model [i.e.  $S1(a)$ ]. On the other hand, plume extension of  $S6(b)$  (i.e. 20-day sub-period) is not compatible with  $S1(a)$  and this shows that the 20-day sub-period is not a suitable sub-period for this problem.

To assess the effect of sub-period length to the result accuracy of this problem, we defined the total mass observed in the aquifer after 2000 days as the basis of accuracy indicator. On this basis, accuracy indicator is defined as follows:

$$Accuracy \% = 100 - \left[ \frac{M_2 - M_1}{M_2} \right] \times 100 \quad (8)$$

where  $M_1$  and  $M_2$  are the amount of mass entered to the aquifer after 2000 days in MODFLOW / MT3DMS and presented model, respectively. Figure 5 shows the accuracy variation versus sub-period length of this problem.

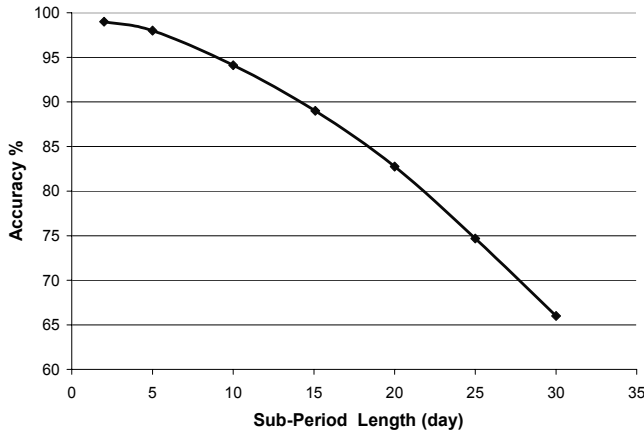


Figure 5. Accuracy variation versus sub-period length.

According to Figure 5, the accuracy of the simulation with presented model using a sub-period less than 5 days is at least 98%. By increasing the length of sub-period, the accuracy would decrease dramatically. For example, by using a 30-day sub-period the accuracy would decrease to 66%. As the result, if a suitable sub-period is selected, it is expected that the simulation will yield to an acceptable engineering solution.

#### 4.2. Application of Both Modules during the Optimization Process

To demonstrate the use of the simulation-optimization model, we simulated a saturated porous medium, 30 m deep, 450 m long, and 350 m wide. The hydraulic conductivity of this medium in all three directions and the effective porosity were assumed to be  $5 \text{ m d}^{-1}$  and 0.5, respectively.

The boundary conditions for the porous medium consist of an upstream constant head equal to 100 m and a downstream constant head boundary equal to 80 m. The predefined contaminant plume in the medium was used as the initial condition and was set equal to 1000 mass units per  $\text{m}^3$ . In addition, a quality constraint is chosen in which the concentration of the contaminant at the end of the remediation period must not exceed 500 mass units per  $\text{m}^3$ . We used a Henry constant ( $H$ ) and a contact coefficient ( $CC$ ) of 0.3 and 0.4, respectively. We specified the use of two existing PAT wells and ten AS wells to remediate the contaminant in this medium. In this case, the construction cost for each PAT well was assumed to be zero. The construction cost of each AS well, the cost of pumping and treatment of each  $1 \text{ m}^3$  of water, and the cost of each  $1 \text{ m}^3$  of air injection were assumed to be 200 000, 250, and 10 currency units, respectively. (These assumptions were based on local costs in Iran.) The boundary conditions, constraint region, initial contaminant plume, and the locations of existing PAT wells and candidate AS wells are shown in

Figure 6. This example is designed in such a way as to predict that AS wells 1 and 6 will be ineffective in the remediation process. In addition, the example will predict that the pumping of PAT well 1 may cause contaminant to flow into the constraint zone whereas pumping by PAT well 2 can prevent this flow.

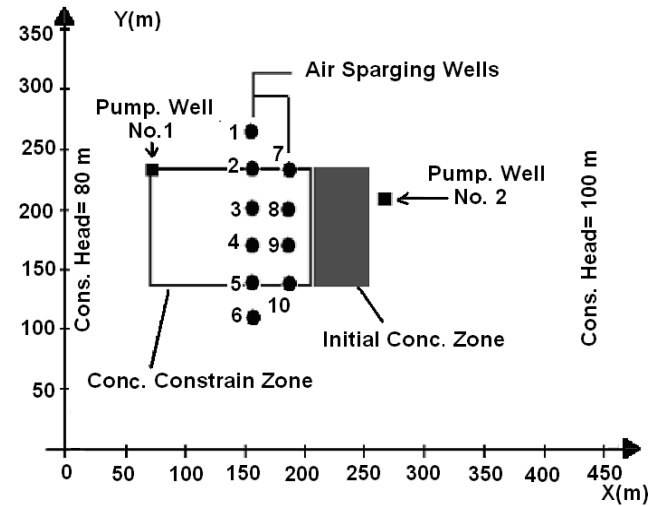


Figure 6. Layout of the optimization problem.

Table 2. Verification of Optimized Answer in Optimization Module

| Question                        | Answer                                 |
|---------------------------------|--|
| Quality constraints satisfied?  | Yes                                    |
| Objective function value?       | 48 600 002                             |
| Pumping rate of PAT well No. 1? | $62 \text{ m}^3 \cdot \text{d}^{-1}$   |
| Pumping rate of PAT well No. 2? | $1426 \text{ m}^3 \cdot \text{d}^{-1}$ |
| Active AS wells?                | 7, 8, and 9                            |
| Shape of chromosome?            | 10000000001110101110                   |

Table 3. Verification of MGO Answer for PAT Remediation

| Question                        | Answer                                 |
|---------------------------------|--|
| Quality constraints satisfied?  | Yes                                    |
| Pumping rate of PAT well No. 1? | $62 \text{ m}^3 \cdot \text{d}^{-1}$   |
| Pumping rate of PAT well No. 2? | $1922 \text{ m}^3 \cdot \text{d}^{-1}$ |
| Objective function value?       | 49 600 000                             |

The allowable interval for the PAT pumping rate was assumed to be between 0 and  $2000 \text{ m}^3 \text{ d}^{-1}$ . In this example, the air injection rate at each AS well was  $3600 \text{ m}^3 \text{ d}^{-1}$ . These AS wells are considered to have only two activation states (on and off), with a constant flow rate under each condition. During the optimization process and when the AS wells are turned off, the construction cost of the AS wells is neglected. The design period, mutation rate, and crossover values used in this example were set to 100 d, 0.02, and 0.2, respectively. The computer used to run this example simulation had a 2 GHz CPU, and took about 3 h to obtain a suitable answer from among 100 generations of possible answers. This answer was obtained in the 84th generation. In addition to using the opti-

mization module, the example was solved using the MGO model for the two existing PAT wells. The results of these two optimizations are compared in Tables 2 and 3.

Plume extensions by the end of design period in the optimized remediation design and the MGO solution are shown in Figures 7 and 8, respectively.

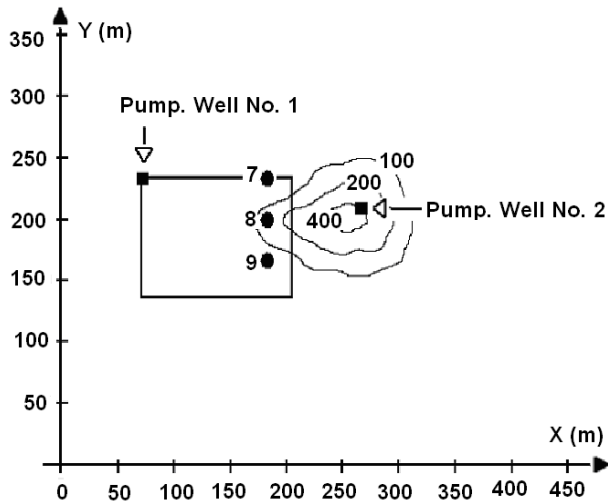


Figure 7. Plume extension in optimization module.

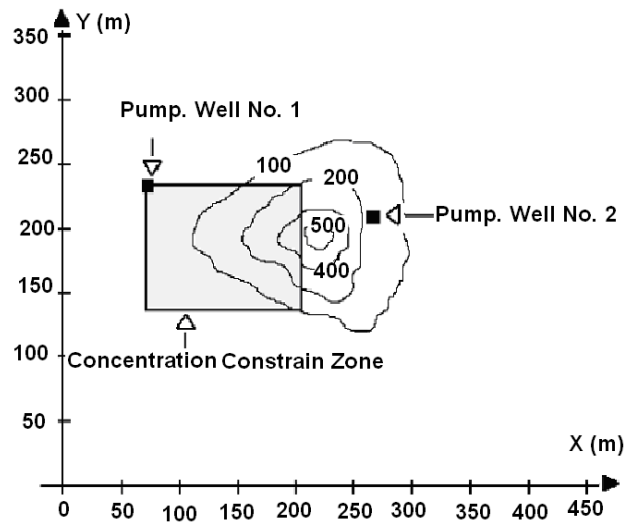


Figure 8. Plume extension in MGO model.

Figure 7 shows that 3 of the 10 candidate AS wells would be sufficient to perform the remediation based on the optimization process. Comparing Tables 2 and 3 shows a clear cost reduction (the objective value) by combining the AS and PAT remediation technologies. Table 2 demonstrates that the cost of remediation would be 48600002. this value is 49600000 in Table 3. This means that, comparing to the MGO solution, the cost of remediation, using optimal solution to the implementation of PAT and AS, would decrease the cost by 2%. Although this rate of decreasing may seem to be small but the

importance of this matter is that the optimization process of the presented model yielded to a solution better than the optimal result of MGO model. According to Table 2, the compliance between predictable result and optimization module result is observed.

### 4.3. Case Study (Field Application of the Simulation Module)

#### 4.3.1. Site and Contamination Specifications

To illustrate the use of the simulation model, we selected a site in the western part of the Tehran Refinery, near the Bagher-Shahr urban areas. Figure 9 shows the position of the site with respect to Tehran. The hydraulic conductivity and aquifer depth at this site are  $5 \text{ m d}^{-1}$  and 30 to 40 m, respectively (TPWSO, 1989). Because the site is near the Tehran Refinery, methyl tertiary-butyl ether (MTBE) has leaked into aquifer during the 1980s and 1990s (DLA, 2005). This compound has been used instead of lead since 1979 as an octane-enhancing additive in gasoline.

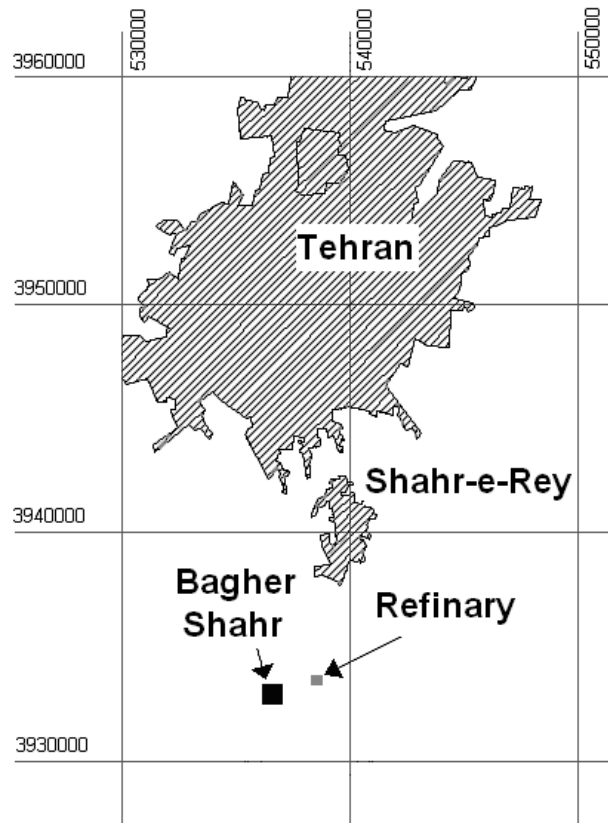


Figure 9. Site location in UTM coordinates.

MTBE is about 30 times as soluble as benzene in water, and is three times as volatile (i.e. its vapor pressure is three times the vapor pressure of benzene). MTBE is much less likely to become adsorbed on soil particles or organic carbon than benzene, and MTBE is more resistant to biological degradation than benzene. Henry's constant for MTBE is about

0.02. To remediate MTBE contamination, both PAT and AS are appropriate approaches (USEPA, 2005). Table 4 shows the concentration of MTBE in some of observation wells of the site. Surveys of the site revealed that the contaminant plume had completely surrounded the urban area (DLA, 2005). The current distribution of the contaminant plume and the boundaries of the urban area are shown in Figure 10.

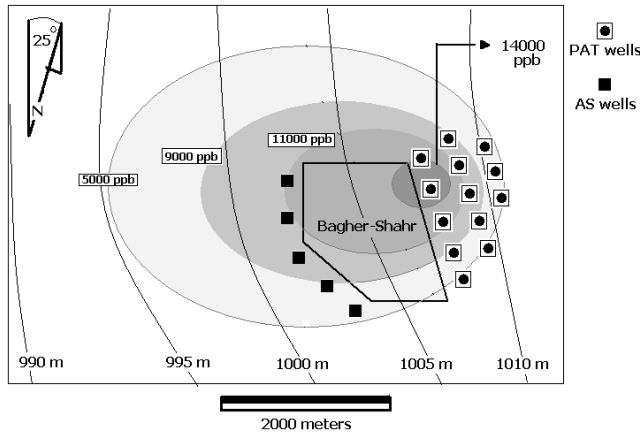


Figure 10. Layout of the case study.

#### 4.3.2. Simulation of the Suggested Remediation Strategy

Based on the type of contaminant and the site characteristics, the AS and PAT technologies are both suitable approaches. The aim of the remediation in both cases is to decrease contaminant concentrations in the urban area without installing remediation equipment in the city (because the installation of remediation equipment is prohibited in urban areas). Based on these goals and constraints, we evaluated the effectiveness of five PAT wells constructed downward the city alone and in combination with a network of AS wells upward the city. In this design, the AS wells would prevent additional entry of contaminant into the city region caused by downstream PAT pumping. The locations of the suggested AS and PAT wells

are shown in Figure 10. The length of the simulation period was set at 5 years and a constant pumping rate of  $2000 \text{ m}^3 \text{ d}^{-1}$  was chosen for the PAT well. For our simulation, we defined a network of 260-m finite-difference cells. The AS wells were verified at the nodes in this model. The air injection rate for the AS wells was set at  $1500 \text{ m}^3 \text{ h}^{-1}$ . Because, in practice, it is not necessary to construct AS wells at nodal positions, more AS wells with less air injection rate could be used to consider the radius of influence of each well. Laboratory data and pilot tests revealed that soil porosity and the contact coefficient between MTBE and air were both 0.2 (DLA, 2005). In addition, we used 2-d sub-periods for the simulation based on preliminary trials, as described in section 2-3.

#### 4.3.3. Simulation Results

Figure 11 shows the final extent of the contaminant plume with no intervention and after implementation of the proposed remediation design after 5 years. Due to slow movement of the groundwater, the contaminant plume shows little change in distribution in the absence of remediation. However, if the proposed remediation strategy is implemented, the hydraulic gradient created by the PAT wells moves the contaminant plume away from the urban area, while the AS wells prevent additional inflow of contaminant into the city area.

Employing the proposed remediation strategy, the total mass of MTBE below the urban area would be decreased to roughly half of its initial value, and the maximum contaminant concentration would decrease to 10,500 ppb, versus about 14,200 ppb if no remediation is performed. The overall MTBE mass balance for this case study is shown in Table 5. According to this table, the suggested PAT and AS arrangement would remove near 46% of total mass in aquifer. The removal rate of PAT and AS would be 152.4 tons and 54.1 tons respectively.

These results illustrate that combining the use of PAT and AS technologies will permit remediation of the contaminated aquifer without requiring the installation of remediation equipment within the urban area. Based on the results of our study, the proposed remediation strategy was approved by the Ira-

Table 4. MTBE Concentration in some of Observation Wells

| Well No. | UTMX   | UTMY    | MTBE (ppb) | Well No. | UTMX   | UTMY    | MTBE (ppb) |
|----------|--------|---------|------------|----------|--------|---------|------------|
| 1        | 538443 | 3934078 | 474        | 10       | 538951 | 3930177 | 5          |
| 2        | 539507 | 3033139 | 52         | 11       | 537847 | 3935408 | 94         |
| 3        | 539573 | 3933547 | 1115       | 12       | 537347 | 3934553 | 1521       |
| 4        | 539985 | 3932910 | 2240       | 13       | 538330 | 3931169 | 612        |
| 5        | 539959 | 3932342 | 4302       | 14       | 537990 | 3930748 | 199        |
| 6        | 539810 | 3932290 | 12         | 15       | 537306 | 3931276 | 5          |
| 7        | 539810 | 3932157 | 62         | 16       | 537121 | 3931215 | 2231       |
| 8        | 539693 | 3933808 | 608        | 17       | 537482 | 3931908 | 4767       |
| 9        | 539935 | 3933534 | 1099       | 18       | 536996 | 3932939 | 15207      |

Table 5. Mass Balance on MTBE at the End of Design Period (unit: ton)

| Initial mass of MTBE | Mass removed by PAT | Mass removed by AS | Total Mass removed | Mass remained |
|----------------------|---------------------|--------------------|--------------------|---------------|
| 451                  | 152.4               | 54.1               | 206.5              | 244.5         |



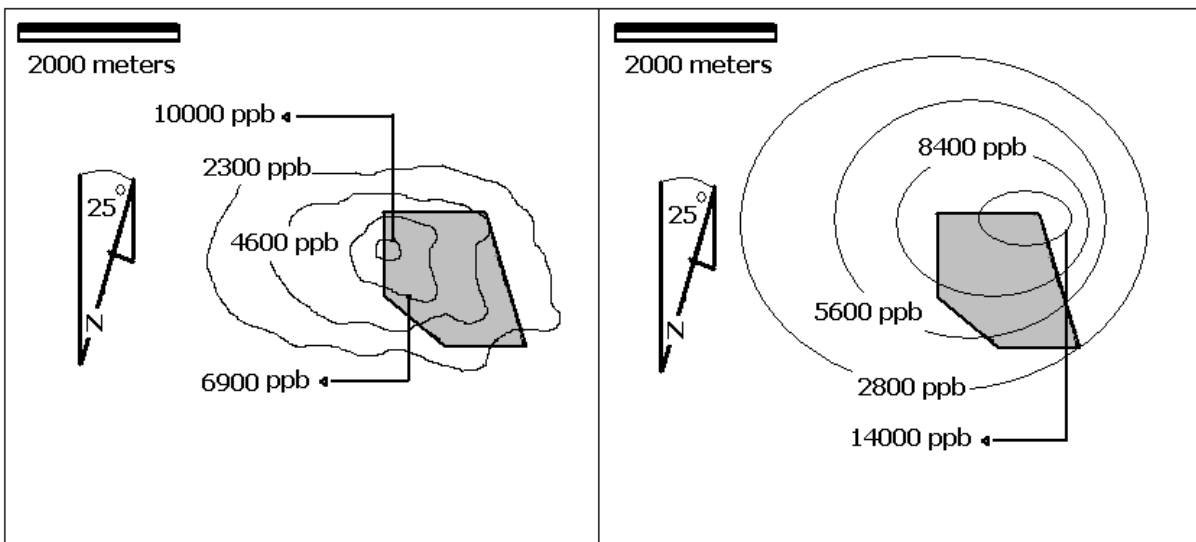


**Figure 11.** Natural extension of MTBE plume (Right) and plume extension when using suggested remediation design (Left).

nian Governmental Organization of Water Management.

## 5. Conclusions

In this study, we describe a simulation-optimization model for modeling the simultaneous use of AS and PAT technologies for remediation of contaminated aquifers. By combining two existing models (MODFLOW and MT3DMS) and incorporating the use of Henry's equation to simulate the use of AS wells, the simulation-optimization model demonstrated significantly increased predictive ability and the possibility for cost savings. The following key results were obtained:

Based on the new concept of sub-period, we could present an efficient model for field scale simulation and optimization of AS and PAT technologies. One of the most important features of this model is that the connection between MODFLOW/MT3DMS model and Henry's equation is automated. To demonstrate capabilities of this model, we implemented both modules of it during some examples and a case study. This model can help engineers, as well as researchers, to simulate and optimize AS and PAT technologies for appropriate sites.

The presented model is stable in respect of hydraulic coefficients and boundary conditions. Our study during an example showed that if an appropriate length for sub-period is selected, then the model will be stable and reliable for field scale application. The presented method of selecting appropriate sub-period may be used for other engineering and research problems.

During the case study and by means of the simulation module of this model, we presented an efficient design to overcome restrictions of remediation for Brgher-Shahr aquifer. We used a specific arrangement of PAT and AS wells. The suggested design showed that it would be possible to remedi-

ate the site without facility installation in urban area. Since the mentioned restrictions are common for remediation of urban areas, the suggested design can be implemented for other scenarios similar to the case study.

## References

- Ahlfeld, D.P., Dahmani, D.W., Johnson, R.L. and Redman, J.D. (1994). Air zone analysis during air sparging, *J. Groundwater Monit. Rem.*, 14(3), 132-139.
- Bass, D.H., Hestings, N.A. and Brown, R.A. (2000). Performance of air sparging systems; a review of case studies, *J. Hazard. Mater.*, 72(2-3), 101-119, doi:10.1016/S0304-3894(99)00136-3.
- Benner, M.L., Stanford, S.M., Lee, L.S. and Mohtar, R.H. (2000). Field and numerical analysis of in-situ air sparging: a case study, *J. Hazard. Mater.*, 72(2-3), 217-236, doi:10.1016/S0304-3894(99)00141-7.
- DLA, Department of Laboratory Affairs of Iranian Environmental Protection Organization (2005). Technical report of strategies for petroleum contamination around Tehran refinery (In Persian), Vol. 2.
- Erickson, M., Mayer, A. and Horn, J. (2002). Multi objective optimal design of groundwater remediation systems; application of Niche-Pareto genetic algorithm, *J. Adv. Water Resour.*, 25, 51-65, doi:10.1016/S0309-1708(01)00020-3.
- Falta, R.W., Pruess, K., Finsterle, S. and Battistelli, A. (1995). *T2VOC User's Guide*, Department of Energy, USA.
- Gen, M. and Cheng, R. (1997). *Genetic Algorithms and Engineering Design*, John Wiley, New York.
- Guan, J. and Aral, M.M. (1999). Optimal remediation with well locations and pumping rates selected as continuous decision variables, *J. Hydrol.*, 221(1), 20-42, doi:10.1016/S0022-1694(99)00079-7.
- Harbaugh, A.W., Banta, E.R., Hill, M. and McDonald, M. (2000). *MODFLOW 2000, the U.S. Groundwater Geological Groundwater Model-User Guide*, USGS, USA.
- Johnson, R.L., Johnson, P.C., McWhorter, D.B. and Hinchee, R.E. (1993). A review of air sparging related topics, *J. Groundwater Monit. Rem.*, 13 (4), 127-135.

- Khan, F.I., Hussain, T. and Hejazi, R. (2004). An overview and analysis of site remediation technologies, *J. Environ. Manage.*, 71(2), 217-236, doi:10.1016/j.jenvman.2004.02.003.
- LaBrecque, D. and Lundergaard, P.D. (1998). Air distribution in semi-homogeneous soil, *First National Conference on Remediation*, pp. 59-71.
- Lesson, A., Hinchee, R.E., Headington, G.L. and Vogel, C.M. (1995). Air distribution in three phase porous media, *Proceeding of the Third International In-Situ and Bioremediation Symposium*, pp. 215-222.
- McCray, J.E. (2000). Mathematical modeling of air sparging for subsurface remediation: state of the art, *J. Hazard. Mater.*, 72, 237-263, doi:10.1016/S0304-3894(99)00142-9.
- McKay, L.J. and Acomb, A. (1996). Air saturation during air injection in porous media, *J. Groundwater Monit. Rem.*, 16(4), 86-94.
- Spiliotopoulos, A.A., Karatzas, D.G. and Pinder, G.F. (2004). A multi period approach to the solution of groundwater management problems using an outer approximation method, *Eur. J. Oper. Res.*, 157(2), 514-525, doi:10.1016/S0377-2217(03)00239-X.
- Thomson, N.R. and Johnson, R.L. (2000). Air distribution during in-situ air sparging: an overview of mathematical modeling, *J. Hazard. Mater.*, 72(2), 265-282, doi:10.1016/S0304-3894(99)00143-0.
- Thomson, R.L., Tomnilson, D.W., Johnson, R.L. and Redman, J.D. (2000). Air and water interaction during air injection in porous media, *J. Hazard. Mater.*, 73, 268-280.
- TPWSO, Tehran Province Water Studies Organization (1989). Geophysics Study of Tehran Aquifer by Electric Method (In Persian).
- USAF (2002). *Air Sparging Design Paradigm*, U.S. Air Force, Armstrong Laboratory, Armstrong, Ohio.
- USEPA (2005). MTBE (methyl tertiary-butyl ether) and underground storage tanks, MTBE Fact Sheet #2. <http://www.epa.gov/oust/mibe>.
- Wang, F.J. and Anderson, M.P. (1982). *Introduction to Groundwater Modeling*, Freeman, San Francisco, CA., USA.
- Zheng, C. and Wang, P. (1999). *Mt3dms: A Modular Three Dimensional Multi Species Transport Model for Simulation of Advection, Dispersion and Chemical Reaction of Contaminants in Groundwater*, U.S. Army Corps of Engineers, USA.
- Zheng, C. and Wang, P. (2002). *A Modular Groundwater Optimizer*, the University of Alabama, Tuscaloosa, Alabama, USA.